

Skeletal Muscle Electrical Stimulation Prevents Progression of Disuse Muscle Atrophy via Forkhead Box O Dynamics Mediated by Phosphorylated Protein Kinase B and Peroxisome Proliferator-Activated Receptor γ Coactivator-1 α

Ayumi TAKAHASHI^{1,2}, Yuichiro HONDA^{1,2}, Natsumi TANAKA³, Jyunpei MIYAKE¹, Shunsuke MAEDA¹, Hideki KATAOKA^{1,4}, Junya SAKAMOTO^{1,2}, Minoru OKITA^{1,2}

¹Department of Physical Therapy Science, Nagasaki University Graduate School of Biomedical Sciences, Nagasaki, Japan, ²Institute of Biomedical Sciences (Health Sciences), Nagasaki University, Nagasaki, Japan, ³Department of Physical Therapy, School of Rehabilitation Sciences, Seirei Christopher University, Hamamatsu, Shizuoka, Japan, ⁴Department of Rehabilitation, Nagasaki Memorial Hospital, Nagasaki, Japan

Received June 11, 2023

Accepted October 12, 2023

Summary

Although electrical muscle stimulation (EMS) of skeletal muscle effectively prevents muscle atrophy, its effect on the breakdown of muscle component proteins is unknown. In this study, we investigated the biological mechanisms by which EMS-induced muscle contraction inhibits disuse muscle atrophy progression. Experimental animals were divided into a control group and three experimental groups: immobilized (Im; immobilization treatment), low-frequency (LF; immobilization treatment and low-frequency muscle contraction exercise), and high-frequency (HF; immobilization treatment and high-frequency muscle contraction exercise). Following the experimental period, bilateral soleus muscles were collected and analyzed. Atrogin-1 and Muscle RING finger 1 (MuRF-1) mRNA expression levels were significantly higher for the experimental groups than for the control group but were significantly lower for the HF group than for the Im group. Peroxisome proliferator-activated receptor γ coactivator-1 α (PGC-1 α) mRNA and protein expression levels in the HF group were significantly higher than those in the Im group, with no significant differences compared to the Con group. Both the Forkhead box O (FoxO)/phosphorylated FoxO and protein kinase B (AKT)/phosphorylated AKT ratios were significantly lower for the Im group than for the control group and significantly higher for the HF group than for the Im group. These results, the suppression of atrogin-1 and MuRF-1 expression for the HF group may be due to decreased nuclear expression of FoxO by AKT phosphorylation and suppression of

FoxO transcriptional activity by PGC-1 α . Furthermore, the number of muscle contractions might be important for effective EMS.

Key words

Electrical muscle stimulation • Disuse muscle atrophy • AKT • PGC-1 α • FoxO

Corresponding author

M. Okita, Institute of Biomedical Sciences (Health Sciences), Nagasaki University, Sakamoto 1-7-1, Nagasaki 852-8520, Japan.
E-mail: mokita@nagasaki-u.ac.jp

Introduction

Disuse muscle atrophy is caused by various factors and leads to deterioration of physical function; the disease results in a restriction of activities of daily living, an increase in medical expenses and nursing care burden, and can even cause mortality [1,2]. Therefore, preventing disuse muscle atrophy is essential for maintaining activities of daily living and quality of life during medical treatment.

Disuse muscle atrophy is caused by immobilization; decreased muscle protein synthesis and enhanced muscle protein degradation are attributable for this condition [3]. In particular, early degradation of muscle component proteins is predominant following immobilization [4-6]. The signaling pathway of the

Forkhead box O (FoxO) family regulates skeletal muscle atrophy [7,8]. The pathway is associated with the ubiquitin-proteasome system, which is involved in the degradation of muscle component proteins [9]. Specifically, FoxO translocates into the nucleus, promotes expression of genes ubiquitin E3 ligases, F-box (MAFbx)/atrogin-1 and muscle RING finger 1 (MuRF-1), and causes skeletal muscle atrophy [10]. FoxO regulation involves phosphorylation by protein kinase B (AKT) and peroxisome proliferator-activated receptor- γ coactivator 1 α (PGC-1 α). AKT is phosphorylated in the insulin-like growth factor 1 (IGF-1)-phosphoinositide 3-kinase (PI3K) pathway upon IGF-1 expression during muscle contractile exercise [10,11]. Phosphorylated AKT (p-AKT) then phosphorylates FoxO, resulting in its translocation to the cytoplasm and subsequent inactivation [12]. PGC-1 α expression is induced through short-duration and long-term exercise [13,14], and represses the transcriptional activity of FoxO leading to the suppression of atrogin-1 and MuRF-1 expression and proteolysis [15-17]. By contrast, in immobilized skeletal muscle, a decrease in p-AKT reduces the amount of phosphorylated FoxO (p-FoxO) in the cytoplasm and markedly increases nuclear FoxO level [1,12,16]. PGC-1 α expression reportedly decreases immediately after skeletal muscle immobilization [17,18]; decreased PGC-1 α expression is associated with muscle atrophy owing to increased FoxO transcriptional activity [17-20]. Thus, changes in expression of p-AKT and PGC-1 α due to skeletal muscle immobilization may be important factors in regulating skeletal muscle mass.

Skeletal muscle tissue metabolism and size of muscle fibers undergo changes in response to altered mechanical loading caused by exercise or immobilization [21,22]. In other words, muscle contractile activity during exercise can be an important means of maintaining skeletal muscle mass. However, exercise may be restricted due to injury or illness. In such cases, electrical muscle stimulation (EMS) is a potentially effective intervention strategy for suppressing skeletal muscle atrophy and increasing muscle mass during disuse [23,24]. Active contraction is important for maintaining skeletal muscles [25,26], and tetanic contractions at 20-50 Hz with EMS have been used in clinical settings to improve skeletal muscle mass and function [27,28]. Muscle atrophy in rat skeletal muscles was prevented by inducing tetanic contractions at 50-100 Hz [26,29]. The molecular mechanisms involved in the inhibitory effect of EMS on muscle atrophy mainly involve activation of the muscle component protein synthesis [22,24]. On the other hand,

EMS mitigates muscle atrophy by inhibiting the degradation of muscle component proteins [30-32]. However, the molecular dynamics of p-AKT and PGC-1 α regarding the FoxO-mediated degradation of these muscle component proteins remain unknown.

Here, we hypothesized that in disuse muscle atrophy, phosphorylated AKT- and PGC-1 α -mediated FoxO dynamics suppress muscle protein degradation during EMS muscle contraction. We tested the hypothesis by applying EMS muscle contraction to rat soleus muscle immediately after immobilization.

Methods

Animals

Eight-week-old male Wistar rats (CLEA Japan Inc., Tokyo, Japan) were maintained at the Center for Frontier Life Sciences at Nagasaki University in 30×40×20-cm cages (two rats/cage) and exposed to a 12-h light-12-h dark cycle at an ambient temperature of 25 °C. Food and water were provided ad libitum. A total of 39 rats (weighing 259.9±11.5 g each) were randomly divided into an experimental group (n=29) and a control group (n=10). The rats in the control group were maintained without treatment or intervention. The ankle joints of rats in the experimental group were subjected to the immobilization process as described in our previous study [33]. Specifically, rats were anesthetized, and a plaster cast was wrapped around both hind limbs from the 2-cm upper part of the patella to the hind paw to keep the ankle joint in full plantar flexion. The experimental group was further divided into immobilized (Im; n=9; immobilization treatment only), low-frequency (LF; n=9; immobilization treatment and muscle contractile exercise with a 2 s (do)/6 s (rest) duty cycle), and high-frequency (HF; n=11; immobilization treatment and muscle contractile exercise with a 2 s (do)/2 s (rest) duty cycle) groups. The experimental protocol was approved by the Ethics Review Committee for Animal Experimentation of Nagasaki University (approval no. 1903281524). All experimental procedures were performed under anesthesia, and efforts were made to minimize suffering.

Protocol for electrical stimulation

Cyclic muscle tetanus contractions were performed using an electrical stimulator (Homer Ion, Tokyo, Japan) as described previously [34]. The belt electrodes were wrapped around the proximal thigh, and the distal lower leg and bilateral lower limb skeletal

muscles were subjected to electrical stimulation with cast removal. Electrical stimulation was applied once daily for six days per week for two weeks. The optimal stimulus intensity and duration of preliminary experiments were determined in accordance with a previous study [34]. Specifically, the electrical frequency was set at 50 Hz to induce tetanic contractions. Stimulus intensity at 100 % maximum voluntary contraction (MVC) was measured, and 60 % MVC (most effective in preventing muscle weakness) was calculated. The results confirmed that 4.7 mA corresponded to 60 % MVC. Stimulation time was identified by measuring plantar flexor muscle strength at a frequency of 50 Hz and stimulation intensity of 4.7 mA. The stimulation was applied until the force reached <2.9 N (60 % MVC). The results showed that plantar flexion muscle force decreased to <2.9 N 28 min and 18 min after the start of electrical stimulation in the LH and HF groups, respectively. Therefore, the stimulation times for the LH and HF groups were set to 20 and 15 min, respectively, as reference times without muscle fatigue.

Tissue sampling and preparation

The rats' left and right soleus muscles were excised 12 h after the final electrical stimulation. After measuring the wet weight of the soleus muscle, samples from the muscles on the right side were embedded in tragacanth gum and frozen in liquid nitrogen. Serial frozen muscle cross-sections were mounted on glass slides for histological analysis. Part of the left soleus muscle was rapidly frozen in liquid nitrogen for western blot analysis. The remaining left soleus muscle was treated with RNAlater® (Ambion, CA, USA) immediately after excision for molecular biological analysis.

Histological analysis

The muscle cross-sections were stained with ATPase (adenosine 5'-triphosphate disodium salt hydrate, Merck KGaA) as described previously [35]. The diameter of each type of myofiber was determined using myofibrillar adenosine triphosphatase (myosin ATPase) staining. A pre-incubation solution (pH 10.8) was used to stain type I and II myofibers in the soleus muscle. The dyed cross-sections of the muscles were evaluated using an optical microscope. The ATPase-stained cross-sectional areas (CSAs) of type I and II myofibers were analyzed using the Scion Image software (National Institutes of Health, MD, USA). More than 100 myofiber measurements were recorded per animal.

Molecular biological analysis

Total RNA was extracted from the soleus muscle using the RNeasy Fibrous Tissue Mini Kit (Qiagen, CA, USA). To prepare cDNA, total RNA was used as a template for the QuantiTect® Reverse Transcription Kit (Qiagen). Real-time polymerase chain reaction (RT-PCR) was performed using Brilliant III Ultra-Fast SYBR Green QPCR Master Mix (Agilent Technologies, CA, USA). The cDNA concentration of all samples was unified to 25 ng/μl; 0.2 μl cDNA was applied to each well. The synthetic gene-specific primers used are listed in Table 1. The threshold cycle (Ct) was determined using the Mx3005P Real-Time QPCR System (Agilent Technologies). The mRNA expression of target genes was calculated using the $\Delta\Delta Ct$ method.

Western blotting

The isolated soleus muscles were subjected to polyacrylamide gel electrophoresis (PAGE) and western blotting. Some soleus muscles were minced and homogenized in ice-cold lysis buffer. The total protein concentration was determined using a BCA Protein Assay Kit (Thermo Scientific, Carlsbad, CA, USA) and adjusted to 2 mg/ml. One-dimensional SDS-PAGE was performed to separate the proteins by molecular weight. After electrophoretic separation, proteins were transferred onto polyvinylidene difluoride membranes. The primary antibodies used were FoxO1 (1:10000; ab1799450, Abcam), phospho-FoxO1 (Ser 319; 1:10000; PA5-37577, Invitrogen), AKT (1:10000; ab233755, Abcam), phospho-AKT (S473; 1:10000; ab81283, Abcam), PGC-1α (1:2000; ab54481, Abcam) and β-actin (1:5000; BioVision; Milpitas, CA, USA). The secondary antibody used were horseradish peroxidase-conjugated anti-rabbit IgG (1:20000; Santa Cruz Biotechnology; Dallas, TX, USA) or anti-mouse IgG (1:20000; Thermo Scientific). The protein bands were detected using ECL SelectTM Western Blotting Detection Reagent (GE Healthcare; Little Chalfont, UK) and Image Quant LAS 500 (GE Healthcare). Band densities were quantified using the Scion Image software (Scion, Frederick, MD, USA).

Statistical analysis

All data are presented as mean ± standard deviation. Differences between groups for other parameters were assessed using one-way Analysis of Variance, followed by Scheffé's method. Differences were considered statistically significant at $p < 0.05$.

Table 1. Sequences of primers used for real-time-polymerase chain reaction.

Object gene	Arrangement		Gene Bank No.
	Forward	Reverse	
<i>Atrogin-1</i>	5'-ACTAAGGAGCGCCATGGATACT-3'	5'-GTTGAATCTTCTGGAATCCAGGAT-3'	AY059628.1
<i>MuRF-1</i>	5'-TGACCAAGGAAACAGCCACCAG-3'	5'-TCACTCTTCTCGTCAGGATGG-3'	AY059627.1
<i>PGC-1α</i>	5'-CAAGCCAACCAACAACCTTATCTCT-3'	5'-CACACTTAAGGTTCGCTCAATAGT-3'	NC051349.1
<i>β-actin</i>	5'-GTGCTATGTTGCCCTAGACTTCG-3'	5'-GATGCCACAGGATTCCATACCC-3'	BC063166.1

PGC, peroxisome proliferator-activated receptor γ coactivator; MuRF, Muscle RING finger.

Table 2. Body weight, muscle wet weight, and ratio of relative weight (muscle wet weight per body weight) of rats after two weeks of immobilization and electrical stimulation.

	Control	Immobilization	LF	HF
<i>BW (g)</i>	285.60 ± 20.77	245.00 ± 10.90*	236.80 ± 13.90*	238.60 ± 10.60*
<i>MWW (mg)</i>	124.71 ± 12.80	69.23 ± 4.94*	61.14 ± 10.13*	62.15 ± 4.56*
<i>RWR (mg/g)</i>	0.43 ± 0.04	0.28 ± 0.02*	0.25 ± 0.04*	0.26 ± 0.02*

BW: body weight, MWW: muscle wet weight, RWR: relative weight ratio, * p<0.05 compared to the control group.

Results

Body weight, muscle wet weight, and ratio of relative weight

Data of body weight, muscle wet weight, and ratio of relative weight (muscle wet weight per body weight) of rats after two weeks of immobilization and electrical stimulation are presented in Table 2. All parameters were significantly lower in the experimental groups than in the control group.

Assessment of the CSAs of type I and II myofibers

Assessment of the CSAs of type I and II myofibers of ATPase-stained cross-sections of the soleus muscle (Fig. 1a) showed that the CSA of type I myofibers for the control group was $2515.65 \pm 249.08 \mu\text{m}^2$ whereas the CSAs for the Im, LF, and HF groups, two weeks after immobilization, were 1295.84 ± 221.88 , 1288.59 ± 188.02 , and $1609.33 \pm 170.68 \mu\text{m}^2$, respectively (Fig. 1b). The CSA of type II myofibers was $1738.46 \pm 158.73 \mu\text{m}^2$ for the control group whereas the CSAs for the Im, LF, and HF groups, two weeks after immobilization were 934.31 ± 94.28 , 942.41 ± 123.07 , and $1050.13 \pm 128.21 \mu\text{m}^2$, respectively (Fig. 1c). The CSAs of type I and II myofibers for the experimental groups were significantly lower than those for the control group. Further, the CSA of type I myofibers for the HF group was significantly higher than the CSAs for the Im or LF groups.

Atrogin-1 and MuRF-1 mRNA expression

The atrogin-1 mRNA expression level for the control group was 0.96 ± 0.26 whereas the levels for the Im, LF, and HF groups, two weeks after immobilization, were 2.93 ± 1.49 , 2.30 ± 0.83 , and 1.85 ± 0.63 , respectively (Fig. 2a). The MuRF-1 mRNA expression level was 1.30 ± 0.30 for the control group whereas the levels for the Im, LF, and HF groups, two weeks after immobilization, were 2.70 ± 1.00 , 2.44 ± 0.85 , and 2.01 ± 0.68 , respectively (Fig. 2b). The expression levels of atrogin-1 and MuRF-1 mRNA were significantly higher for the experimental groups than for the control group. Further, the levels for the HF group were significantly lower than those for the Im or LF groups.

PGC-1α mRNA and protein expression

The level of PGC-1α mRNA expression was 0.93 ± 0.15 for the control group whereas the levels for the Im, LF, and HF groups, two weeks after immobilization, were 0.39 ± 0.11 , 0.58 ± 0.08 , and 0.99 ± 0.24 , respectively (Fig. 2c). The level of PGC-1α mRNA expression for the Im and LF groups was significantly lower than that for the control group. The expression of PGC-1α mRNA in the HF group was significantly higher than that in the Im group, with no significant differences compared to the Con group. The level of PGC-1α protein in the soleus muscle was quantified (Fig. 2d). The level of expression of PGC-1α protein was 0.34 ± 0.13 for the control group

whereas the Im, LF, and HF groups, two weeks after immobilization, were 0.09 ± 0.04 , 0.18 ± 0.03 , and 0.33 ± 0.16 , respectively (Fig. 2e). The PGC-1 α protein expression for the HF group were significantly higher than those in Im group and no significantly differences with Con group.

Expression of FoxO1 and p-FoxO1 proteins

The levels of total FoxO1 and p-FoxO1 proteins in the soleus muscle were quantified (Fig. 3a). The total expression level of FoxO1 protein was 0.62 ± 0.40 for the control group whereas the levels for the Im, LF, and HF groups, two weeks after immobilization, were 0.62 ± 0.32 , 0.60 ± 0.20 , and 0.62 ± 0.28 , respectively (Fig. 3b). The level of p-FoxO1 protein expression was 0.17 ± 0.12 for the control group whereas the levels for the Im, LF, and HF groups, two weeks after immobilization, were 0.09 ± 0.05 , 0.11 ± 0.03 , and 0.16 ± 0.10 , respectively (Fig. 3c). The ratio of FoxO1/p-FoxO1 protein expression was 3.89 ± 1.07 for the control group whereas the ratios for the Im, LF, and HF groups, two weeks after immobilization, were 7.37 ± 2.03 , 5.42 ± 1.77 , and 4.32 ± 1.29 , respectively (Fig. 3d). The ratio of FoxO1/p-FoxO1 protein expression for the Im group was significantly higher than that for the control group. Further, the ratio of FoxO1/p-FoxO1 protein expression for the HF group was significantly lower than for the Im group. The ratio of p-FoxO1/FoxO1 protein expression was 0.27 ± 0.07 for the control group whereas

the ratios for the Im, LF, and HF groups, two weeks after immobilization, were 0.14 ± 0.03 , 0.21 ± 0.09 , and 0.25 ± 0.09 , respectively (Fig. 3e). The ratio of p-FoxO1/FoxO1 protein expression for the Im group was significantly lower than that for the control group. Further, the HF group showed a significantly higher ratio of p-FoxO1/FoxO1 protein expression than the Im group.

Expression of AKT and p-AKT protein

The levels of total AKT and p-AKT in the soleus muscle were quantified (Fig. 4a). The total level of expression of AKT protein was 0.99 ± 0.45 for the control group whereas the levels for the Im, LF, and HF groups, two weeks after immobilization, were 0.89 ± 0.25 , 1.05 ± 0.35 , and 0.88 ± 0.29 , respectively (Fig. 4b). The level of p-AKT protein expression was 1.02 ± 0.49 for the control group whereas the levels for the Im, LF, and HF groups, two weeks after immobilization, were 0.39 ± 0.15 , 0.68 ± 0.28 , and 0.79 ± 0.33 , respectively (Fig. 4c). The level of p-AKT protein expression for the Im group was significantly lower than that for the control group. The ratio of p-AKT/AKT protein expression was 1.10 ± 0.38 for the control group whereas the ratios for the Im, LF, and HF groups, two weeks after immobilization, were 0.49 ± 0.28 , 0.67 ± 0.27 , and 0.92 ± 0.29 , respectively (Fig. 4d). The ratio of p-AKT/AKT protein expression for the Im group was significantly lower than that for the control group. Further, the HF group showed a significantly higher ratio of p-AKT/AKT protein expression than the Im group.

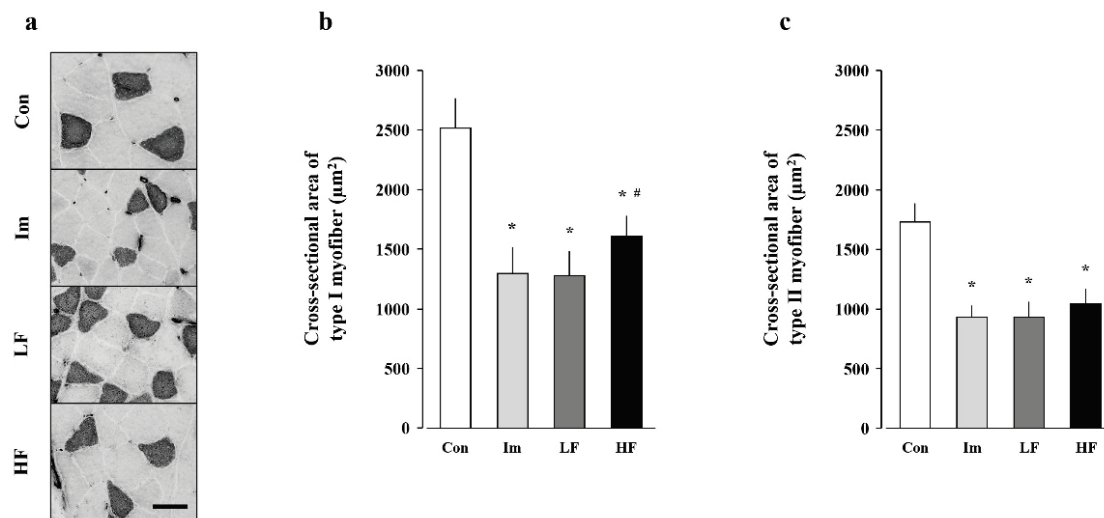


Fig. 1. ATPase-stained cross-sectional areas (CSAs) of type I and II myofibers in the soleus muscle. **(a)** ATPase staining of the soleus muscle. White areas, type I fibers. Black areas, type II fibers. Scale bar, 50 μ m. **(b)** CSA of type I fibers. **(c)** CSA of type II fibers. Open bars, control group (con). Light gray bars, Im group. Dark gray bars, LF group. Black bars, HF group. Data are presented as mean \pm standard deviation. * Significant difference ($p<0.05$) compared with the control group. # Significant difference ($p<0.05$) compared with the Im group. † Significant difference ($p<0.05$) compared with the LF group. Im, immobilization; LF, low-frequency; HF, high-frequency.

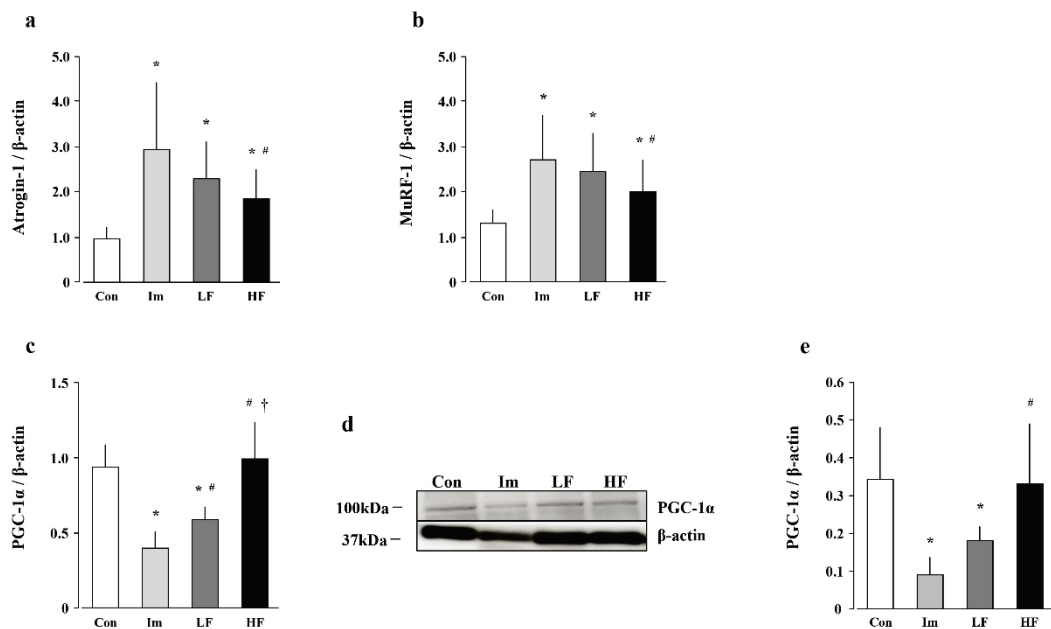


Fig. 2. mRNA expression of atrogin-1, MuRF-1, and PGC-1 α and protein expression of PGC-1 α in the soleus muscle. mRNA expression of atrogin-1 (**a**), MuRF-1 (**b**), and PGC-1 α (**c**) in the soleus muscle. Quantification of PGC-1 α (**d**) and western blot detection of PGC-1 α and β -actin (**e**). Open bars, control group (con). Light gray bars, Im group. Dark gray bars, LF group. Black bars, HF group. Data are presented as mean \pm standard deviation. *Significant difference ($p<0.05$) compared with the control group. #Significant difference ($p<0.05$) compared with the Im group. †Significant difference ($p<0.05$) compared with the LF group. Im, immobilization; LF, low-frequency; HF, high-frequency.

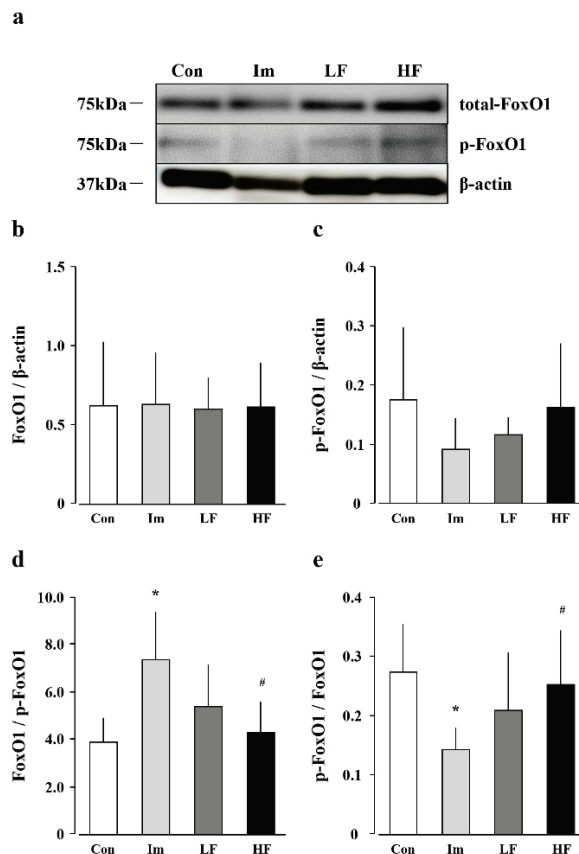


Fig. 3. Protein expression of Forkhead box O (FoxO1) and phosphorylated FoxO1 (p-FoxO1) in the soleus muscle. Quantification of total FoxO1 and p-FoxO1 (**a**) in the soleus muscle. Western blot detection of FoxO1 (**b**), p-FoxO1 (**c**), and β -actin. The ratios of FoxO1/p-FoxO1 (**d**), p-FoxO1/ FoxO1 (**e**). Open bars, control group (con). Light gray bars, Im group. Dark gray bars, LF group. Black bars, HF group. Data are presented as mean \pm standard deviation. *Significant difference ($p<0.05$) compared with the control group. #Significant difference ($p<0.05$) compared with the Im group. Im, immobilization; LF, low-frequency; HF, high-frequency.

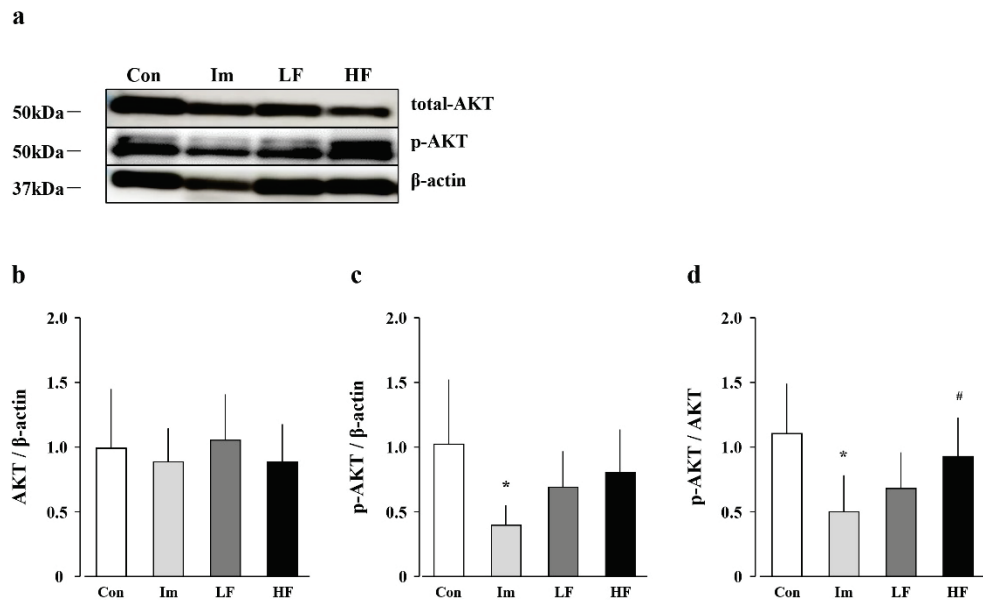


Fig. 4. Protein expression of protein kinase B (AKT) and phosphorylated AKT (p-AKT) and in the soleus muscle. Quantification of total AKT and p-AKT (**a**) in the soleus muscle. Western blot detection of AKT (**b**), p-AKT (**c**), and β-actin. The ratios of p-AKT/AKT (**d**). Open bars, control group (con). Light gray bars, Im group. Dark gray bars, LF group. Black bars, HF group. Data are presented as mean ± standard deviation. * Significant difference ($p<0.05$) compared with the control group. # Significant difference ($p<0.05$) compared with the Im group. Im, immobilization; LF, low-frequency; HF, high-frequency.

Discussion

The degradation of muscle component proteins during the early stages of disuse is an important contributor to the development and progression of muscle atrophy, and strategies to prevent this process are required. This study aimed to determine whether p-AKT- and PGC-1α-mediated FoxO dynamics suppress muscle component protein degradation during EMS muscle contraction exercise in disuse muscle atrophy. In the following subsections, the mechanisms underlying muscle atrophy due to immobility and the effects of electrical stimulation on muscle atrophy are discussed.

Immobilization increases the breakdown of muscle component proteins in the soleus muscle, leading to progressive disuse muscle atrophy

In the present study, immobilization caused a decrease in skeletal muscle mass and CSA in type I and type II fibers and increased the expression of atrogin-1 and MuRF-1. Immobilization promoted the degradation of muscle constituent proteins *via* the ubiquitin-proteasome system due to the increased expression of atrogin-1 and MuRF-1, causing a decrease in muscle mass and CSA. Previous studies using immobilized and hindlimb fixation models have shown that muscle mass and CSA are significantly reduced in the soleus muscle

[21,36,37]. The ubiquitin-proteasome system is considered a major proteolytic pathway during muscle fiber atrophy and is involved in the accelerated degradation of muscle component proteins [9]. The E3 ubiquitin ligases atrogin-1 and MuRF-1 are expressed at low levels in normal skeletal muscle but are rapidly induced in immobilized muscle and serve as key factors leading to muscle atrophy [1,9].

The AKT/FoxO and PGC-1α/FoxO pathways are involved in the enhanced degradation of muscle component proteins in skeletal muscle immobilization

In this study, expression of p-AKT and p-FoxO proteins as well as that of PGC-1α mRNA were reduced in the soleus muscles of rats in the Im group compared to the control group. These changes, occurring due to the immobilization of skeletal muscle, caused increased nuclear expression and transcriptional activity of FoxO, which led to increased expression of atrogin-1 and MuRF-1 and finally resulted in accelerated degradation of muscle component proteins. Specifically, FoxO has been reported to migrate to the nucleus and induce muscle atrophy by promoting increased expression of atrogin-1 and MuRF1 [9]. p-AKT promotes the nuclear exclusion and cytoplasmic retention of FoxO and regulates its nuclear expression [3,8]. However, immobilization of skeletal muscle decreases the phosphorylation of AKT by

attenuating phosphorylation signals from the IGF-1/PI3K pathway, and promotes the degradation of muscle component proteins by inducing dephosphorylation of FoxO and increasing its nuclear expression [7]. Furthermore, the transcriptional activity of FoxO has been shown to correlate with PGC-1 α . Previous reports have shown that, in denervation following muscle atrophy, FoxO transcriptional activity increases in response to reduced PGC-1 α expression, promoting a decrease in skeletal muscle mass [17,20]. In addition, mRNA levels of PGC-1 α were found to be significantly reduced in immobilized models whereas mRNA levels of atrogin-1 and MuRF1 were found to be increased [38]. Therefore, it can be inferred that increased nuclear expression of FoxO due to decreased phosphorylation of AKT, and increased transcriptional activity due to decreased expression of PGC-1 α , contributed to the progression of disuse muscle atrophy in the Im group in this study by promoting the degradation of muscle component proteins of the ubiquitin-proteasome system.

High-frequency muscle contraction exercise induced by electrical stimulation prevents the decrease of CSA of immobilized soleus muscle

The present study showed no significant differences in CSA between the LF and Im groups. In contrast, atrophy of the type I CSA muscle was lower for the HF group compared to that for the Im or LF groups. Because the number of muscle contraction exercises per day was 150 and 225 for the LF and HF group, respectively, it was inferred that the high-frequency of muscle contraction exercises by electrical stimulation suppressed the decrease in the CSA of the immobilized soleus muscle. Previous studies have reported that EMS attenuates disuse atrophy in the soleus muscle [39,40] and that the efficiency of EMS depends on the frequency and intensity of stimulation as well as the duration and number of contractions [40]. Further, the number of muscle contractions per day affects the optimal maintenance of muscle mass, with a minimum of 200 contractions per day being required [41].

EMS with a high frequency of muscle contraction exercise promotes phosphorylation of AKT and expression of PGC-1 α

In the present study, the HF group expressed more p-AKT than the Im group, which mitigated the reduction in p-FoxO expression. This was presumed to indicate reduced nuclear FoxO expression. The beneficial

effects of EMS on muscle atrophy are attributed to the molecular responses occurring in skeletal muscles [2]. Electrical stimulation of the skeletal muscle promotes AKT phosphorylation [42]. p-AKT phosphorylates FoxO, which translocates to the cytoplasm leading to a reduced expression in the nucleus [12,42]. In this study, PGC-1 α mRNA and protein expression was significantly lower in the Im and LF groups compared with the Con group. However, both expressions of PGC-1 α in the HF group were significantly higher than those in the Im group, with no significant differences with Con group. These results indicate that muscle contraction exercise in the HF group prevented the decrease in PGC-1 α expression caused by immobilization. It has been previously shown that repeated muscle contraction exercise induces PGC-1 α expression [13,14]. Furthermore, local overexpression of PGC-1 α suppresses the transcriptional activity of FoxO in disuse muscle atrophy [18] and suppresses the expression of Atrogin-1 and MuRF-1 [17]. Based on the above, we speculate that frequent electrically-stimulated muscle contraction exercise inhibits the progression of disuse muscle atrophy by enhancing AKT phosphorylation and PGC-1 α expression and suppressing the increase in nuclear transcriptional activity of FoxO associated with immobilization.

Limitations

This study has several limitations. First, it remains to be determined whether the EMS stimulation conditions used in this study were the most effective. Further investigation is needed because electrical stimulation conditions may vary in effectiveness with different frequencies, intensities, duty cycles, duration, and daytime sessions. In addition, the present study showed efficacy only in type I CSA but could not explain this phenomenon. Therefore, a detailed validation based on muscle fiber type is required. Furthermore, data on the causal relationship between cellular and molecular events needs to be comprehensive. Future studies using antagonists or inhibitors are warranted to address these limitations.

Conclusions

Suppression of nuclear expression of FoxO associated with AKT phosphorylation and the transcriptional activity of FoxO via PGC-1 α may halt the progression of disuse muscle atrophy. Furthermore, the

number of muscle contractions might be important for effective EMS.

Conflict of Interest

There is no conflict of interest.

Acknowledgements

This research was supported by the Japan Society for the Promotion of Science (KAKENHI, Grant No. 21H03291, 23K19928) and ALCARE Co. Ltd. (Tokyo, Japan). The belt electrode-skeletal muscle electrical stimulation system was provided by Homer Ion Co. Ltd. (Tokyo, Japan).

References

1. Rudrappa SS, Wilkinson DJ, Greenhaff PL, Smith K, Idris I, Atherton PJ. Human Skeletal Muscle Disuse Atrophy: Effects on Muscle Protein Synthesis, Breakdown, and Insulin Resistance-A Qualitative Review. *Front Physiol* 2016;7:361. <https://doi.org/10.3389/fphys.2016.00361>
2. Graham ZA, Lavin KM, O'Bryan SM, Thalacker-Mercer AE, Buford TW, Ford KM, Broderick TJ, ET AL. Mechanisms of exercise as a preventative measure to muscle wasting. *Am J Physiol Cell Physiol* 2021;321:C40-C57. <https://doi.org/10.1152/ajpcell.00056.2021>
3. Mukund K, Subramaniam S. Skeletal muscle: A review of molecular structure and function, in health and disease. *Wiley Interdiscip Rev Syst Biol Med* 2020;12:e1462. <https://doi.org/10.1002/wsbm.1462>
4. Thomason DB, Booth FW. Atrophy of the soleus muscle by hindlimb unweighting. *J Appl Physiol* (1985) 1990;68:1-12. <https://doi.org/10.1152/jappl.1990.68.1.1>
5. Phillips SM, McGlory C. CrossTalk proposal: The dominant mechanism causing disuse muscle atrophy is decreased protein synthesis. *J Physiol* 2014;592:5341-5343. <https://doi.org/10.1113/jphysiol.2014.273615>
6. Atherton PJ, Greenhaff PL, Phillips SM, Bodine SC, Adams CM, Lang CH. Control of skeletal muscle atrophy in response to disuse: clinical/preclinical contentions and fallacies of evidence. *Am J Physiol Endocrinol Metab* 2016;311:E594-E604. <https://doi.org/10.1152/ajpendo.00257.2016>
7. Sanchez AM, Candau RB, Bernardi H. FoxO transcription factors: their roles in the maintenance of skeletal muscle homeostasis. *Cell Mol Life Sci* 2014;71:1657-1671. <https://doi.org/10.1007/s00018-013-1513-z>
8. Chen K, Gao P, Li Z, Dai A, Yang M, Chen S, Su J, ET AL. Forkhead Box O Signaling Pathway in Skeletal Muscle Atrophy. *Am J Pathol* 2022;192:1648-1657. <https://doi.org/10.1016/j.ajpath.2022.09.003>
9. Vainshtein A, Sandri M. Signaling Pathways That Control Muscle Mass. *Int J Mol Sci* 2020;21:4759. <https://doi.org/10.3390/ijms21134759>
10. Bonaldo P, Sandri M. Cellular and molecular mechanisms of muscle atrophy. *Dis Model Mech* 2013;6:25-39. <https://doi.org/10.1242/dmm.010389>
11. Yoshida T, Delafontaine P. Mechanisms of IGF-1-Mediated Regulation of Skeletal Muscle Hypertrophy and Atrophy. *Cells* 2020;9:1970. <https://doi.org/10.3390/cells9091970>
12. Stitt TN, Drujan D, Clarke BA, Panaro F, Timofeyva Y, Kline WO, Gonzalez M, ET AL. The IGF-1/PI3K/Akt pathway prevents expression of muscle atrophy-induced ubiquitin ligases by inhibiting FOXO transcription factors. *Mol Cell* 2004;14:395-403. [https://doi.org/10.1016/S1097-2765\(04\)00211-4](https://doi.org/10.1016/S1097-2765(04)00211-4)
13. Baar K, Wende AR, Jones TE, Marison M, Nolte LA, Chen M, Kelly DP, ET AL. Adaptations of skeletal muscle to exercise: rapid increase in the transcriptional coactivator PGC-1. *FASEB J* 2002;16:1879-1886. <https://doi.org/10.1096/fj.02-0367com>
14. Russell AP, Feilchenfeldt J, Schreiber S, Praz M, Crettenand A, Gobelet C, Meier CA, ET AL. Endurance training in humans leads to fiber type-specific increases in levels of peroxisome proliferator-activated receptor-gamma coactivator-1 and peroxisome proliferator-activated receptor-alpha in skeletal muscle. *Diabetes* 2003;52:2874-2881. <https://doi.org/10.2337/diabetes.52.12.2874>
15. Brault JJ, Jespersen JG, Goldberg AL. Peroxisome proliferator-activated receptor gamma coactivator 1alpha or 1beta overexpression inhibits muscle protein degradation, induction of ubiquitin ligases, and disuse atrophy. *J Biol Chem* 2010;285:19460-19471. <https://doi.org/10.1074/jbc.M110.113092>

16. Allen DL, Bandstra ER, Harrison BC, Thorng S, Stodieck LS, Kostenuik PJ, Morony S, ET AL. Effects of spaceflight on murine skeletal muscle gene expression. *J Appl Physiol* (1985) 2009;106:582-595. <https://doi.org/10.1152/japplphysiol.90780.2008>
17. Cannavino J, Brocca L, Sandri M, Bottinelli R, Pellegrino MA. PGC1- α over-expression prevents metabolic alterations and soleus muscle atrophy in hindlimb unloaded mice. *J Physiol* 2014;592:4575-4589. <https://doi.org/10.1113/jphysiol.2014.275545>
18. Kang C, Ji LL. PGC-1 α overexpression via local transfection attenuates mitophagy pathway in muscle disuse atrophy. *Free Radic Biol Med* 2016;93:32-40. <https://doi.org/10.1016/j.freeradbiomed.2015.12.032>
19. Sandri M, Lin J, Handschin C, Yang W, Arany ZP, Lecker SH, Goldberg AL, ET AL. PGC-1alpha protects skeletal muscle from atrophy by suppressing FoxO3 action and atrophy-specific gene transcription. *Proc Natl Acad Sci U S A* 2006;103:16260-16265. <https://doi.org/10.1073/pnas.0607795103>
20. Qin W, Pan J, Wu Y, Bauman W, Cardozo C. Protection against dexamethasone-induced muscle atrophy is related to modulation by testosterone of FOXO1 and PGC-1a. *Biochem Biophys Res Commun* 2010;403:473-478. <https://doi.org/10.1016/j.bbrc.2010.11.061>
21. Booth FW, Gollnick PD. Effects of disuse on the structure and function of skeletal muscle. *Med Sci Sports Exerc* 1983;15:415-420. <https://doi.org/10.1249/00005768-198315050-00013>
22. Mirzoev TM. Skeletal Muscle Recovery from Disuse Atrophy: Protein Turnover Signaling and Strategies for Accelerating Muscle Regrowth. *Int J Mol Sci* 2020;21:7940. <https://doi.org/10.3390/ijms21217940>
23. Jones S, Man WD, Gao W, Higginson IJ, Wilcock A, Maddocks M. Neuromuscular electrical stimulation for muscle weakness in adults with advanced disease. *Cochrane Database Syst Rev* 2016;10:CD009419. <https://doi.org/10.1002/14651858.CD009419.pub3>
24. Maffiuletti NA, Green DA, Vaz MA, Dirks ML. Neuromuscular Electrical Stimulation as a Potential Countermeasure for Skeletal Muscle Atrophy and Weakness During Human Spaceflight. *Front Physiol* 2019;10:1031. <https://doi.org/10.3389/fphys.2019.01031>
25. Nader GA, Esser KA. Intracellular signaling specificity in skeletal muscle in response to different modes of exercise. *J Appl Physiol* (1985) 2001;90:1936-1942. <https://doi.org/10.1152/jappl.2001.90.5.1936>
26. Dow DE, Faulkner JA, Dennis RG. Distribution of rest periods between electrically generated contractions in denervated muscles of rats. *Artif Organs* 2005;29:432-435. <https://doi.org/10.1111/j.1525-1594.2005.29086.x>
27. Doucet BM, Lam A, Griffin L. Neuromuscular electrical stimulation for skeletal muscle function. *Yale J Biol Med* 2012;85:201-215. <https://doi.org/10.1016/j.yeulekin.2011.12.005>
28. Sillen MJ, Franssen FM, Gosker HR, Wouters EF, Spruit MA. Metabolic and structural changes in lower-limb skeletal muscle following neuromuscular electrical stimulation: a systematic review. *PLoS One* 2013;8:e69391. <https://doi.org/10.1371/journal.pone.0069391>
29. de Freitas GR, Santo CCDE, de Machado-Pereira NAMM, Bobinski F, Dos Santos ARS, Ilha J. Early Cyclical Neuromuscular Electrical Stimulation Improves Strength and Trophism by Akt Pathway Signaling in Partially Paralyzed Biceps Muscle After Spinal Cord Injury in Rats. *Phys Ther* 2018;98:172-181. <https://doi.org/10.1093/ptj/pzx116>
30. Russo TL, Peviani SM, Durigan JL, Gigo-Benato D, Delfino GB, Salvini TF. Stretching and electrical stimulation reduce the accumulation of MyoD, myostatin and atrogin-1 in denervated rat skeletal muscle. *J Muscle Res Cell Motil* 2010;31:45-57. <https://doi.org/10.1007/s10974-010-9203-z>
31. Dupont E, Cieniewski-Bernard C, Bastide B, Stevens L. Electrostimulation during hindlimb unloading modulates PI3K-AKT downstream targets without preventing soleus atrophy and restores slow phenotype through ERK. *Am J Physiol Regul Integr Comp Physiol* 2011;300:R408-R417. <https://doi.org/10.1152/ajpregu.00793.2009>
32. Dirks ML, Wall BT, Snijders T, Ottenbros CL, Verdijk LB, van Loon LJ. Neuromuscular electrical stimulation prevents muscle disuse atrophy during leg immobilization in humans. *Acta Physiol (Oxf)* 2014;210:628-641. <https://doi.org/10.1111/apha.12200>
33. Oga S, Goto K, Sakamoto J, Honda Y, Sasaki R, Ishikawa K, Kataoka H, ET AL. Mechanisms underlying immobilization-induced muscle pain in rats. *Muscle Nerve* 2020;61:662-670. <https://doi.org/10.1002/mus.26840>

34. Honda Y, Tanaka N, Kajiwara Y, Kondo Y, Kataoka H, Sakamoto J, Akimoto R, ET AL. Effect of belt electrode-skeletal muscle electrical stimulation on immobilization-induced muscle fibrosis. PLoS One 2021;16:e0244120. <https://doi.org/10.1371/journal.pone.0244120>
35. Hintz CS, Coyle EF, Kaiser KK, Chi MM, Lowry OH. Comparison of muscle fiber typing by quantitative enzyme assays and by myosin ATPase staining. J Histochem Cytochem 1984;32:655-660. <https://doi.org/10.1177/32.6.6202737>
36. Ohira Y, Yoshinaga T, Nomura T, Kawano F, Ishihara A, Nonaka I, Roy RR, ET AL. Gravitational unloading effects on muscle fiber size, phenotype and myonuclear number. Adv Space Res 2002;30:777-781. [https://doi.org/10.1016/S0273-1177\(02\)00395-2](https://doi.org/10.1016/S0273-1177(02)00395-2)
37. Zhong H, Roy RR, Siengthai B, Edgerton VR. Effects of inactivity on fiber size and myonuclear number in rat soleus muscle. J Appl Physiol (1985) 2005;99:1494-1499. <https://doi.org/10.1152/japplphysiol.00394.2005>
38. Wang J, Wang F, Zhang P, Liu H, He J, Zhang C, Fan M, ET AL. PGC-1 α over-expression suppresses the skeletal muscle atrophy and myofiber-type composition during hindlimb unloading. Biosci Biotechnol Biochem 2017;81:500-513. <https://doi.org/10.1080/09168451.2016.1254531>
39. Canon F, Goubel F, Guezennec CY. Effects of chronic low frequency stimulation on contractile and elastic properties of hindlimb suspended rat soleus muscle. Eur J Appl Physiol Occup Physiol 1998;77:118-124. <https://doi.org/10.1007/s004210050309>
40. Boonyarom O, Kozuka N, Matsuyama K, Murakami S. Effect of electrical stimulation to prevent muscle atrophy on morphologic and histologic properties of hindlimb suspended rat hindlimb muscles. Am J Phys Med Rehabil 2009;88:719-726. <https://doi.org/10.1097/PHM.0b013e31818e02d6>
41. Dow DE, Cederna PS, Hassett CA, Kostrominova TY, Faulkner JA, Dennis RG. Number of contractions to maintain mass and force of a denervated rat muscle. Muscle Nerve 2004;30:77-86. <https://doi.org/10.1002/mus.20054>
42. Valero-Breton M, Warnier G, Castro-Sepulveda M, Deldicque L, Zbinden-Foncea H. Acute and Chronic Effects of High Frequency Electric Pulse Stimulation on the Akt/mTOR Pathway in Human Primary Myotubes. Front Bioeng Biotechnol 2020;8:565679. <https://doi.org/10.3389/fbioe.2020.565679>